Electronic structure of transition-metal tetracoordinated complexes 4.* Theoretical *ab initio* and UV-photoelectron spectroscopy study of nickel(II) and palladium(II) complexes of *N*,*N'*-1,3-propaneaminebis(1H-pyrrol-2-ylmethylene) Schiff base

Enrico Ciliberto, Santo Di Bella, Antonino Gulino** and **Ignazio L. Fragalà**
Dipartimento di Scienze Chimiche, Università di Catania, viale A. Doria 8, 95125 Catania (Italy)

(Received May 3, 1990; revised July 2, 1990)

Abstract

Structural and bonding properties of the Ni and Pd complexes of the title Schiff base have been studied with the aid of both the pseudopotential *ab initio* method, in partial geometry optimizations, for investigation of ground-state electronic structure and for evaluation of ionization energies, and of He I/He II photoelectron spectroscopy. Theoretical results have provided an accurate description of metal–ligand bonding. It appears dominated by σ interactions involving the upper lying MOs mainly N_{2p} lone pair in character and, though to a different extent, valence metal subshells. Despite the different functionalities existing in the ligand chromophore, comparable bonding properties, and hence similar Pd–N distances, have been found for the four nitrogen donor atoms. A theoretical explanation of this behaviour is provided. Low ionization energy structures of photoelectron spectra have been assigned in accordance with ΔSCF calculations.

Introduction

Chemical and structural peculiarities of transition-metal complexes with Schiff base ligands have been extensively studied [1–5]. In particular *N*-alkylaminebis(1H-pyrrol-2-ylmethylene) and related ligands (Scheme 1) form a vast class of complexes [6–10] which are neutral, monomeric, rather volatile and, depending on the nature of the N-alkyl substituents, may be planar or tetrahedral [2, 11–13]. Despite the breadth of studies on Schiff base transition-metal complexes [1–5], only a limited number of theoretical investigations devoted to the understanding of their electronic structure has been reported as yet [14–16].

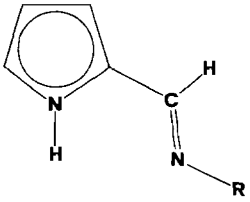

Scheme 1.

As a part of an extensive study on the electronic structure of metal d^8 square-planar complexes [17–19], in this paper we report on the *N*,*N'*-1,3-propaneaminebis(1H-pyrrol-2-ylmethylene) (H_2L) ligand and on its planar Pd(II) and Ni(II) complexes (Scheme 2). The present study represents a case investigation of tetradentate Schiff base complexes with a N_4 coordinating framework having two different donor functionalities and combines an experimental photoelectron (PE) spectroscopy approach using variable (He I and He II) photon sources with pseudopotential *ab initio* calculations for ground-state electronic properties, partial geometry optimization and ΔSCF evaluation of ionization energies (*IE*s).

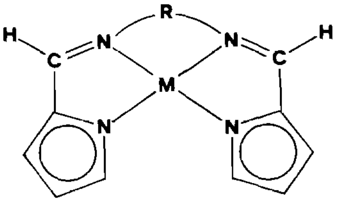

R=μ-(CH$_2$)$_3$; M=Ni, Pd

Scheme 2.

---

*For Part 3 see ref. 19.
**Author to whom correspondence should be addressed.

The calculations were performed on the model molecules *N*-methylaminebis(1H-pyrrol-2-ylmethylene) (HL′) (Fig. 1) and Pd(L′)$_2$ (Fig. 2). The models adopted represent the best combination for both accurate studies of metal–ligand interactions and simplification of computational efforts [16].

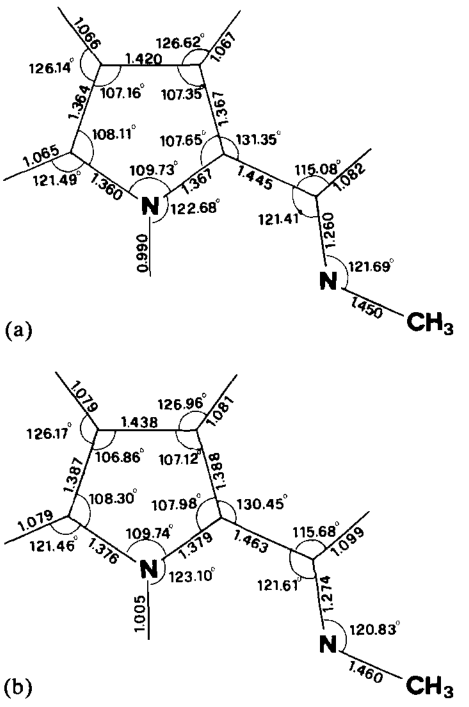

Fig. 1. Optimized geometries of the model HL′: (a) 4-31G standard basis sets; (b) ECP calculations.

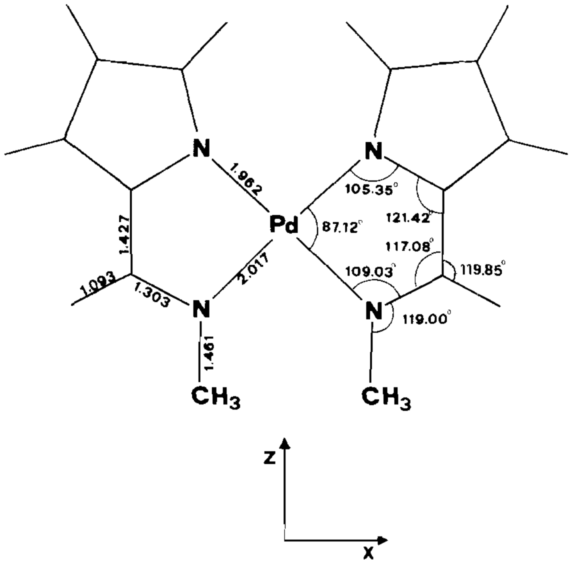

Fig. 2. Optimized geometrical parameters of the model Pd(L′)$_2$ complex.

Experimental

The preparative routes to the H$_2$L ligand and to its M(L) complexes (M = Ni, Pd) have already been reported [7]. Prior to the PE measurements, all the compounds were purified by sublimation *in vacuo*. The complexes gave satisfactory mass spectrometric analyses [10].

PE spectra were recorded with the aid of a photoelectron spectrometer interfaced to an IBM PC AT computer as described elsewhere [17, 18]. Procedures used to 'lock' the energy scale to defined internal references have also been described previously [17, 18]. Spectral resolution measured on the Ar$^+$ $^2P_{3/2}$ peak was always better than 0.030 eV.

Computational details

ab initio Effective core potentials (ECPs) gradient calculations were used for geometry optimizations. The relativistic ECPs and bases of Hay and Wadt [20] were used for Pd. The ECPs and sp bases of Stevens *et al.* [21] were adopted for C and N atoms and Dunning's basis set [22] for H atoms. Valence Gaussian basis sets were always contracted in a double-zeta quality. Ionization energies and other molecular properties were evaluated through pseudopotential [23, 24] restricted Hartree–Fock *ab initio* calculations [17, 18] on optimized geometries using literature parameters [25, 26]. Contracted valence basis sets of double-zeta quality were used as described elsewhere [17, 18]. Calculations were performed by using the HONDO [27] and PSHONDO [28] codes implemented on an IBM 9370 computer.

The geometry of the model HL′ subunit was fully optimized using both 4-31G standard basis sets and ECP calculations. Optimizations were always said to be convergent when the maximum gradient was less than 1×10^{-3} Hartree/a.u.

Both methods point to quite similar geometrical parameters (Fig. 1) thus indicating the validity of the ECP method for geometry optimizations. In particular the structure of the HL′ molecule shows a planar geometry (C_s symmetry) with a more stable *s-trans* conformation (4.95 Kcal/mol) than the *s-cis* conformer. This data agrees well with previous NMR studies on heterocyclic azomethines [29].

The structure of Pd(L) is not known, therefore the geometry of the model Pd(L′)$_2$ complex (Fig. 2) was optimized. All parameters were optimized except those of the pyrrole rings. They were taken from the optimized parameter of the HL′ model. A planar starting geometry (C_{2v} symmetry) was assumed as found in the X-ray structure of the [*N,N*′-

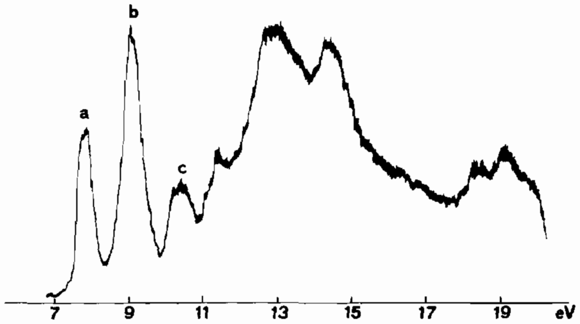

Fig. 3. He I PE spectrum of H_2L.

ethylenebis(pyrrol-2-ylmethyleneaminato)]Ni complex [12].

Results and discussion

Qualitatively, the H_2L ligand can be described as formed by two non-interacting HL′ subunits whose electronic valence structures might be discussed in the simpler terms of perturbations due to *N*-methylenemethylamine ($CH_3{-}N{=}CH{-}$) α-substituent upon the topmost molecular orbitals (MOs) of a simple pyrrole ring [30]. Therefore the topmost MOs of H_2L must consist of twinned orbitals representing the three π systems of the pyrrole ring, the imine in-the-plane nitrogen lone pair (n_i) and, finally, the π MO associated to the C=N bond.

Eigenvalues and population analysis of uppermost MOs of HL′ are reported in Table 1. MO composition data agrees well with the proposed qualitative description and, in particular, the almost pure pyrrole character of 4a″ (π_3) and 5a″ (π_4) MOs appears indicative of the anticipated minor π interactions between the pyrrole ring and the imine α-substituent.

The low *IE* region (< 11 eV) of the PE spectrum of H_2L is shown in Fig. 3. It consists of three well resolved bands (a–c) whose relative intensity ratios are roughly 1:2:1. The assignment (Table 1) can be safely based on perturbative and ΔSCF *IE* data since theoretical values fit experimental *IE*s and intensity data well. Furthermore the proposed assignment agrees well with *IE* literature data of pyrrole [30] and of *N*-benzylidenemethylamine [31], and, worthy of note, the absence of any evident splitting (within the present experimental resolution) associated to bands a, b and c is evidence of the expected lack of significant interactions between the two HL′ units.

M(L) complexes (M = Ni, Pd) possess planar structures and constrained *cis* configurations due to an *N,N*′-alkyl bridging group [2, 12]. The results of ground-state calculations for the model $Pd(L')_2$ are reported in Table 2. They may be better considered in comparison to those for the $(L')_2{}^{2-}$ cluster dianion (Table 3) which, in turn, are close counterparts of valence MOs of H′L (Table 1) once the new $16a_1$ and $16b_1$, almost pure in-the-plane pyrrole N_{2p} lone pairs (n_p) are taken into account as an effect of the deprotonation process. Worthy of note too is the minor admixture of n_p and n_i lone pair MOs (Table 3).

Population analysis of $Pd(L')_2$ (Table 2) shows that metal 4d, 5s and 5p orbitals are strongly admixed with a large part of ligand valence MOs. In particular, those of π symmetry ($d_{yz,xy}$) appear strongly admixed with the $3b_2$ and $3a_2$ (π_2 C=N in character) ligand MOs to form the $3b_2$–$4b_2$ and $3a_2$–$4a_2$ MOs respectively. By contrast the $5b_2$, $5a_2$ (π_3) and the $6b_2$, $6a_2$ (π_4) MOs maintain in the complex their original pyrrole character because they are only slightly perturbed by the bonded metal atom. Moreover σ interactions due to filled $4d_{z^2,x^2-y^2}$ metal orbitals involve, to various extent, almost all ligand MOs of suitable symmetry. As a matter of fact, the major metal–ligand bonding interaction involves the virtual Pd $4d_{xz}$ and $5p_{x,z}$ and the ligand $15b_1$ (n_i), and $16b_1$, $16a_1$ (n_p) MOs respectively. Thus, the formation of $15b_1$ and of $16b_1$, $17a_1$ MOs is the major source of energetic stabilization of Pd(L). Furthermore, it is worthy of note that, at variance to that found in $(L')_2{}^{2-}$, the n_p and n_i lone pair MOs strongly admix together and with deeper σ MOs through the metal

TABLE 1. PSHONDO eigenvalues, computed *IE*s and population analysis of the model HL′ and PE data of H_2L

MO	Eigenvalue −(eV)	*IE* (eV)			Population[a] (%)						Character
		ΔSCF	PT[b]	Exp.[c]	N_i	N_p	C_i	C_p	CH_3	H	
5a″	7.94	7.49	7.60	7.90 (a)	13		1	84	2		π_4
4a″	9.52	8.77	8.83	9.06 (b)		32		68			π_3
16a′	10.81	8.83	8.84		68		5	3	14	10	n_i
3a″	11.96		11.29	10.48 (c)	30	4	36	14	16		π_2

[a] i and p subscripta refer to imine and pyrrole atoms, respectively. [b] PT = perturbative treatment (see ref. 17). [c] Labels refer to spectral features in Fig. 3.

TABLE 2. PSHONDO eigenvalues and population analysis of outermost MOs of the model $Pd(L')_2$

MO	Eigenvalue −(eV)	Population[a] (%)									Overlap population[a]		Dominant character
		Pd			N_i	N_p	C_i	C_p	CH_3	H	Pd–N_i	Pd–N_p	
		4d	5s	5p									
$6a_2$	7.45	1			16			82	1		−0.008	0.000	π_4
$6b_2$	7.50	2			16			82			−0.010	0.000	π_4
$5a_2$	8.33	6				33		61			0.000	−0.034	π_3, d_{xy}
$5b_2$	8.65	3				34	1	62			0.000	−0.012	π_3
$18a_1$	10.48	59	16		7	10		4	1	3	0.028	0.038	$d_{x^2-y^2}$, d_{z^2}
$4b_2$	11.59	34			20	2	16	24	4		−0.044	−0.014	π_2, d_{yz}
$16b_1$	11.66			5	29	32	2	19	8	5	0.054	0.068	n_i, n_p
$4a_2$	11.81	18			26	6	28	8	14		−0.040	0.022	π_2, d_{xy}
$17a_1$	12.17	2		7	27	28	2	16	10	8	0.034	0.058	n_i, n_p
$3a_2$	12.98	51			5	6		35	3		0.032	−0.028	d_{xy}, π_2
$16a_1$	13.59	57			4	6	1	25		7	0.022	−0.036	$d_{x^2-y^2}$, d_{z^2}
$15b_1$	13.62	7			12	5	3	46	12	15	0.035	0.010	σ, d_{xz}
$3b_2$	13.93	50			21	1	11	3	14		0.054	0.014	d_{yz}, π_2
$15a_1$	14.03	13			5	1	6	62	5	8	0.002	0.006	σ, d_{z^2}

	$4d_{x^2-y^2}$	$4d_{z^2}$	$4d_{xy}$	$4d_{xz}$	$4d_{yz}$	5s	$5p_x$	$5p_y$	$5p_z$
Metal orbital population	1.926	1.954	1.974	0.650	1.981	0.421	1.93	0.026	0.191

	Pd	N_i	N_p	C_i	$\bar{C}_p$		Pd–N_i	Pd–N_p
Atomic charge[a]	+0.683	−0.545	−0.458	+0.203	−0.087	Overlap population[a]	+0.410	+0.468

[a] i and p subscripta refer to imine and pyrrole atoms, respectively.

TABLE 3. PSHONDO eigenvalues and population analysis of outermost MOs of the ligand dianion $(L')_2{}^{2-}$

MO	Eigenvalue (eV)	Population[a] (%)						Character
		N_i	N_p	C_i	C_p	CH_3	H	
$5a_2$	0.75	16	2		81	1		π_4
$5b_2$	0.61	15	2		81	2		π_4
$4a_2$	0.01		36		64			π_3
$4b_2$	−0.20		35		65			π_3
$16b_1$	−1.01	3	74		20		3	n_p
$15b_1$	−2.31	70	3	4	2	11	10	n_i
$16a_1$	−2.41	8	66		20		6	n_p
$15a_1$	−3.39	62	8	4	6	12	8	n_i
$3a_2$	−3.70	30	3	32	26	9		π_2
$3b_2$	−3.99	33	4	31	26	6		π_2

[a] i and p subscripta refer to imine and pyrrole atoms, respectively.

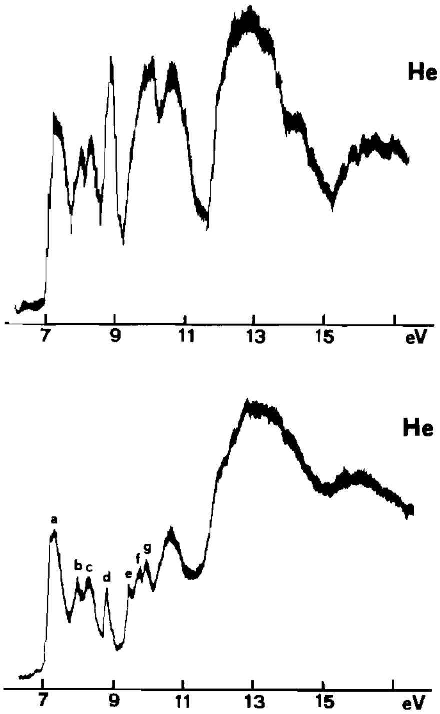

Fig. 4. He I and He II PE spectra of Pd(L).

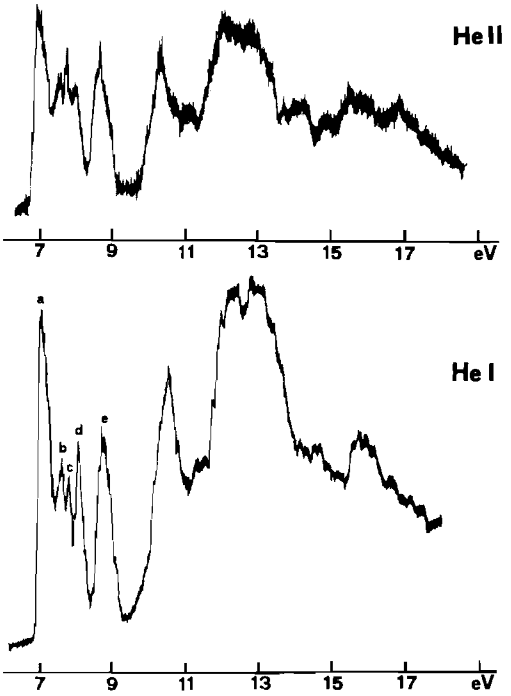

Fig. 5. He I and He II PE spectra of Ni(L).

$5p_\sigma$ and $4d_\sigma$ intermediacy (Tables 2, 3) thus resulting in similar Pd–N_p and Pd–N_i total overlap population values (Table 2) and rather small differences (0.055 Å) in optimized Pd–N_p and Pd–N_i distances (Fig. 2). Overall, this data agrees well with other experimental evidence: structural data of the related *N,N'*-ethyleneamine Ni complex [12], XPS data of the same complex showing that both N_p and N_i atoms have similar electronic environments [32] and, finally, with the average M–N distances found in X-ray structures of several Pd square-planar complexes containing five-membered chelating rings [2].

The PE spectrum of Pd(L) is shown in Fig. 4. It is shaped differently to that of H_2L. Seven well-resolved structures (a–g) can be detected in the region up to 10 eV. Significant variations of relative intensities are observed upon switching to He II excitation. In particular the intensities of band d, and, though moderately, that of the e–g envelope, increase relative to bands a–c (Fig. 4). The assignment of these low *IE* features can be readily made on the basis of computed *IE* values (Table 4).

Bands a, b and c, are assigned to ionizations from the almost degenerate pair $6b_2+6a_2$ (π_4), and $5a_2$ (π_3) and $5b_2$ (π_3) MOs, respectively. The small 0.33

TABLE 4. Experimental *IE*s, computed IEs[a] and assignments of PE Spectra of Pd(L) and Ni(L)

Band label	Pd(L)				Ni(L)	
	IE (eV)			Assignment[c]	*IE* (eV) Exp.	Assignment
	Exp.	ΔSCF	PT[b]			
a	7.22	6.97 7.06	7.18 7.26	$6a_2$ $6b_2$	7.07	$6a_2$ $6b_2$
b	7.89	7.69	7.88	$5a_2$	7.60	$5a_2$
c	8.22	8.03	8.21	$5b_2$	7.83	$18a_1$
d	8.70	8.10	8.30	$18a_1$	8.09	$5b_2$
e	9.28		10.65	$4b_2$	8.71	$4b_2$, $16b_1$
f	9.66		10.67	$16b_1$		$4a_2$
g	9.80		10.98	$4a_2$		

[a] Computed IEs refer to the model compound $Pd(L')_2$. [b] Perturbative values take into account repolarization contributions scaled by a 0.75 factor (see ref.17). [c] See Table 2.

eV *IE* splitting of bands b and c can be hardly associated to differential Pd–N interactions involving d_π metal- and π_3-related ligand based orbitals (Table 2) whereas it likely depends upon through-space non-bonded interactions even operating in the ligand dianion system (Table 3). Furthermore, the considerably lower *IE* shifts (~ 0.7 eV) of bands a–c relative to corresponding ionizations in H_2L (bands a, b) are likely to be due to some antibonding destabilization of corresponding MOs as well as to the enhanced negative charge on the ligand framework (0.68 e.u.) due to the metal-to-ligand charge transfer upon the complex formation (Table 2).

Next, band d is certainly associated to the ionization of the $18a_1$ MO, and, the dramatic enhancement of its relative intensity in the He II spectrum (Fig. 4) accords well with the dominant metal 4d character (Table 2) [18]. Finally, bands e–g are assigned to $(4b_2)^{-1}$, $(16b_1)^{-1}$ and $(4a_2)^{-1}$ ionizations. They become slightly more intense in the He II spectrum in accordance with the 18 and 34% metal 4d contributions in the $4a_2$ and $4b_2$ MOs, respectively (Table 2).

The PE spectrum of Ni(L) (Fig. 5) presents analogies with that of the Pd complex (Fig. 4) thus suggesting an analogous assignment (Table 4). It consists of five well resolved bands (a–e) up to 9 eV. In particular bands a–d find close counterparts in the spectrum of Pd(L). The associated lower *IE* shifts (Table 4) seem to be indicative of an enhanced negative charge on the ligand framework. The e–g envelope in the spectrum of Pd(L) now coalesce in the single band e whose *IE* appears considerably shifted to a lower value. Finally, an evident intensity increase of band c is observed in the He II spectrum (Fig. 5). Therefore, this band can be confidently assigned to the ionization of the MO dominated by the $d_{x^2-y^2}$, d_{z^2} contributions ($18a_1$ MO in $Pd(L')_2$). Of course, this implies an inverted sequence of ionizations corresponding to the $(5b_2)^{-1}$ and $(18a_1)^{-1}$ ionizations (Table 4) and, hence, a greater (than in Pd(L)) energy splitting (0.49 eV) between the $5b_2$ and $5a_2$ π_3 MOs. This observation might be indicative of some preferential interaction with d_π metal orbitals in addition to possibly enhanced through-space interactions depending upon the smaller metal radius and, therefore, upon a smaller Ni–N distances.

Conclusions

The *ab initio* ECP gradient method has proven suitable for geometry optimizations of such large complexes containing heavy atoms with relatively low computational efforts. Furthermore ΔSCF and perturbative *IE*s have provided an adequate rationale for the low *IE* features of the PE spectrum of Pd(L).

In accordance with the previous studies of other square-planar complexes [17–19] the metal–ligand bonding appears strongly dominated by σ interactions involving almost all the upper filled ligand MOs and metal nd_σ, $(n+1)s$, and $(n+1)p_\sigma$ orbitals. They are responsible for an appreciable ligand-to-metal charge transfer. Metal–ligand π interactions involve only the π_2 (C=N) ligand based MOs. The π_3 and π_4 MOs maintain in the complex an almost pure pyrrole character.

Theoretical results show comparable bonding properties, and hence similar Pd–N overlap populations and Pd–N distances, of both the imine- and the pyrrole-nitrogen donor atoms. The metal nd_σ and $(n+1)p_\sigma$ intermediacy, in fact, strongly admix the n_i and n_p N_{2p} lone pairs. The nitrogen donor atoms, therefore behave as a symmetric N_4 chromophore.

Acknowledgements

We thank the Consiglio Nazionale delle Ricerche (CNR, Rome) and the Ministero della Pubblica Istruzione (MPI, Rome) for financial support.

References

1 R. H. Holm, G. W. Everett, Jr. and A. Chakravorty, *Prog. Inorg. Chem., 7* (1966) 83.
2 R. H. Holm and M. J. O'Connor, *Prog. Inorg. Chem., 14* (1971) 241.
3 H. S. Maslen and T. N. Waters, *Coord. Chem. Rev., 17* (1975) 137.
4 S. Yamada and A. Takeuchi, *Coord. Chem. Rev., 43* (1982) 187.
5 A. Syamal and M. R. Maurya, *Coord. Chem. Rev., 95* (1989) 183.
6 R. H. Holm, A. Chakravorty and L. J. Theriot, *Inorg. Chem., 5* (1966) 625.
7 J. H. Weber, *Inorg. Chem., 6* (1967) 258.
8 K.-N. Yeh and R. H. Barker, *Inorg. Chem., 6* (1967) 830.
9 R. E. Clarke and J. H. Weber, *J. Inorg. Nucl. Chem., 30* (1968) 1837.
10 C. J. Jones and J. A. McCleverty, *J. Chem. Soc. A,* (1971) 1052.
11 C. H. Wei, *Inorg. Chem., 11* (1972) 1100.
12 C. Kabuto, T. Kikuchi, H. Yokoi and M. Iwaizumi, *Chem. Lett.,* (1984) 573.
13 H. P. Jensen, *Transition Met. Chem., 10* (1985) 307.
14 C. Daul, C. W. Schapfer and A. von Zelewsky, *Struct. Bonding (Berlin), 36* (1979) 129.
15 J. M. Fernandez-G., M. J. Rosales-Hoz, M. F. Rubio-Arroyo, R. Salcedo, R. A. Toscano and A. Vela, *Inorg. Chem., 26* (1987) 349.
16 R. Colle, A. Fortunelli, N. Re and O. Salvetti, *J. Am. Chem. Soc., 110* (1988) 8016.
17 S. Di Bella, I. Fragalà and G. Granozzi, *Inorg. Chem., 25* (1986) 3997.
18 S. Di Bella, M. Casarin, I. Fragalà, G. Granozzi and T. J. Marks, *Inorg. Chem., 27* (1988) 3993.
19 E. Ciliberto, S. Di Bella, I. Fragalà, G. Granozzi, N. A. Burton, I. H. Hillier, J. Kendrick and M. F. Guest, *J. Chem. Soc., Dalton Trans.,* (1990) 849.
20 P. J. Hay and W. R. Wadt, *J. Chem. Phys., 82* (1985) 270.
21 W. J. Stevens, H. Basch and M. Krauss, *J. Chem. Phys., 81* (1984) 6026.
22 T. H. Dunning, *J. Chem. Phys., 53* (1970) 2823.
23 J. C. Barthelat, Ph. Durand and A. Serafini, *Mol. Phys., 33* (1977) 159.
24 M. Pélissier and Ph. Durand, *Theor. Chim. Acta, 55* (1980) 43.
25 Molecular *ab initio* calculations using pseudopotential, *Laboratoire de Physique Quantique, Toulouse, Tech. Rep.,* 1981.
26 J. P. Daudey, G. Jeung, M. E. Ruiz and O. Novaro, *Mol. Phys., 46* (1982) 67.
27 M. Dupuis, J. D. Watts, H. O. Villar and G. J. B. Hurst, *HONDO: Version 7.0,* Documentation, IBM Corporation, Kingston, New York, 1988.
28 Pseudopotential adaptation (J. P. Daudey) of HONDO 76; M. Dupuis, J. Rys and H. F. King, *QCPE, 11* (1977) 338.
29 F. A. Bottino, M. L. Longo, D. Sciotto and M. Torre, *Can. J. Chem., 59* (1981) 1205.
30 L. Klasinc, A. Sabljic, G. Kluge, J. Rieger and M. Scholz, *J. Chem. Soc., Perkin Trans., 2* (1982) 539.
31 T. Bally, E. Haselbach, S. Lanyova, F. Marschner and M. Rossi, *Helv. Chim. Acta, 59* (1976) 468.
32 J. G. Dillard and L. T. Taylor, *J. Electron Spectrosc. Relat. Phenom., 3* (1974) 455.